Report

Activity-Independent Prespecification of Synaptic Partners in the Visual Map of *Drosophila*

P. Robin Hiesinger,[1,2,8,9,*] R. Grace Zhai,[1,2,8] Yi Zhou,[1,2]
Tong-Wey Koh,[3] Sunil Q. Mehta,[3] Karen L. Schulze,[1,2]
Yu Cao,[2] Patrik Verstreken,[1,2] Thomas R. Clandinin,[5]
Karl-Friedrich Fischbach,[6] Ian A. Meinertzhagen,[7]
and Hugo J. Bellen[1,2,3,4,*]
[1] Howard Hughes Medical Institute
[2] Department of Molecular and Human Genetics
[3] Program in Developmental Biology
[4] Department of Neuroscience
Baylor College of Medicine
Houston, Texas 77030
[5] Department of Neurobiology
Stanford University
Stanford, California 94305
[6] Institute for Biology III
University of Freiburg
D-79104 Freiburg
Germany
[7] Neuroscience Institute and Department of Psychology
Life Sciences Centre
Dalhousie University
Halifax, Nova Scotia B3H 4J1
Canada

Summary

Specifying synaptic partners and regulating synaptic numbers are at least partly activity-dependent processes during visual map formation in all systems investigated to date [1–5]. In *Drosophila,* six photoreceptors that view the same point in visual space have to be sorted into synaptic modules called cartridges in order to form a visuotopically correct map [6, 7]. Synapse numbers per photoreceptor terminal and cartridge are both precisely regulated [8–10]. However, it is unknown whether an activity-dependent mechanism or a genetically encoded developmental program regulates synapse numbers. We performed a large-scale quantitative ultrastructural analysis of photoreceptor synapses in mutants affecting the generation of electrical potentials (*norpA, trp;trpl*), neurotransmitter release (*hdc, syt*), vesicle endocytosis (*synj*), the trafficking of specific guidance molecules during photoreceptor targeting (*sec15*), a specific guidance receptor required for visual map formation (*Dlar*), and 57 other novel synaptic mutants affecting 43 genes. Remarkably, in all these mutants, individual photoreceptors form the correct number of synapses per presynaptic terminal independently of cartridge composition. Hence, our data show that each photoreceptor

forms a precise and constant number of afferent synapses independently of neuronal activity and partner accuracy. Our data suggest cell-autonomous control of synapse numbers as part of a developmental program of activity-independent steps that lead to a "hardwired" visual map in the fly brain.

Results and Discussion

To understand the cellular mechanisms that ensure synapse formation between visuotopically correct partners in the visual map of the fly brain, we performed a comprehensive quantitative ultrastructural analysis of mutants affecting different aspects of synapse formation and function. The fly's compound eye is an assembly of ~750 modules or ommatidia. Each ommatidium contains six outer photoreceptors (R1–R6) that terminate in the first optic neuropil, the lamina, to form a primary visual map [9]. The lamina is arguably one of the best-characterized synaptic regions of any brain: all cell types and synapses, including their precise number and distribution, are well known from serial electron microscopy (EM) reconstructions [8–10]. Neighboring points in visual space are mapped onto neighboring synaptic modules, or cartridges. Each cartridge contains six photoreceptor terminals that receive input from a single point in space but originate from six different ommatidia according to the principle of neural superposition [6, 7]. A disruption of this precise arrangement leads to a loss of the visuotopic map and optomotor behavior [6, 11]. The axons of the central photoreceptors of each ommatidium, R7 and R8, traverse the lamina and establish a regular retinotopic array of terminals in two separate layers of the second optic neuropil, the medulla. In this study we focus on the specification and formation of the synapses formed by R1–R6 in the lamina.

Neuronal Activity Is Not Required for Synaptic Partner Selection, Synapse Formation, or Refinement of Synapse Numbers in Photoreceptors

First, we investigated the developmental requirement for neuronal activity. Electrical activity in developing fly photoreceptors has been shown to occur in mid-pupal [12] and late-pupal [13] stages. We analyzed a panel of mutants (Figure 1A) that disrupt (1) the generation of electrical potentials: $norpA^{p24}$ (phospholipase C, required for phototransduction [14]) and $trp^{343};trpl^{302}$ (Ca^{2+} channels, required for evoked [15] as well as spontaneous [16] generation of electrical potentials); (2) the conduction of electrical potentials: $para^{ts1}$ (Na^+ channel, required to propagate graded potentials) as well as tetrodotoxin (TTX) injection during development (see Supplemental Data available online); and (3) the release of neurotransmitter: hdc^{jk910} (histidine decarboxylase, required to synthesize histamine, the neurotransmitter in photoreceptor required for vision [17, 18]) and *synaptotagmin* (syt^{AD4}; a Ca^{2+}-sensor required for neurotransmitter release [19]).

*Correspondence: robin.hiesinger@utsouthwestern.edu (P.R.H.); hbellen@bcm.edu (H.J.B.)
[8] These authors contributed equally to this work.
[9] Present address: Department of Physiology and Green Center Division for Systems Biology, UT Southwestern Medical Center at Dallas, Dallas, Texas 75390.
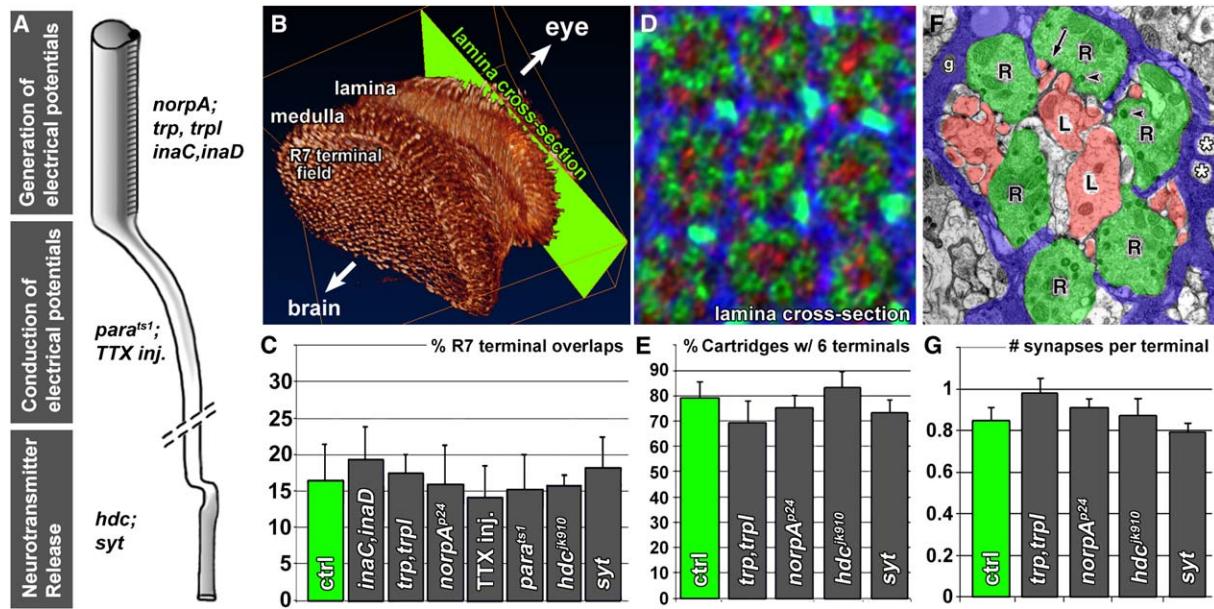
Figure 1. Reverse Genetics: Neuronal Activity Mutants Display No Defects in Photoreceptor Synapse Specification

(A) Selection of mutants that affect the generation or conduction of electrical potentials or neurotransmitter release. The tetrodotoxin (TTX) injection experiment is described in Supplemental Data.

(B) 3D visualization of photoreceptor axon projections in the fly brain based on an antibody staining with the photoreceptor-specific antibody mAb 24B10 against Chaoptin [31]. Note the regular pattern of the R7 terminal field viewed from inside the brain.

(C) Quantification of R7 terminal overlaps in all mutants including TTX injection flies reveals no fine-structural alterations (cf. Figure S1).

(D and E) Quantification of the cartridge organization in lamina cross-sections (cf. [B]) reveals normal R1–R6 sorting in those mutants affecting the generation of electrical potentials or neurotransmitter release (cf. Figure S2). The antibody combination used in (D) labels R1–R6 (green), postsynaptic lamina-monopolar cells (red), and cartridge-enwrapping epithelial glia (blue) as previously described [20].

(F and G) Ultrastructural investigation reveals no alteration of the number of synapses formed in the same mutants (cf. Figure S4). Error bars are SEM.

We first assessed axon targeting in all mutants and found no obvious defects in the ability of R1–R6 to target the lamina or R7/R8 to target separate layers in the medulla (Figure S1). To examine fine-structural alterations more closely, we analyzed R7 terminals, because the normal regularity of R7 projections facilitates the identification of even very subtle defects in the pattern of the terminals and their filopodial interactions (Figure 1B; Figure S1) [20]. We found no obvious defects in any mutant or in TTX-treated animals (Figure 1C; Figure S1). We previously reported that mutations in *neuronal synaptobrevin (n-syb)* affect R7 filopodial fine structure either because of a developmental role of neurotransmitter release or an unknown early developmental role of *n-syb* [21]. Our data now indicate that this developmental requirement for *n-syb* is independent of evoked or spontaneous activity, Ca²⁺-dependent release, as well as the neurotransmitter required for vision. Consistent with these findings, we and others found a developmental function of n-Syb in fly photoreceptors that is independent of neurotransmitter release ([22], P.R.H. and H.J.B., unpublished observations).

We next investigated the axon projection patterns of the outer photoreceptors R1–R6 in the lamina by visualizing the cartridge organization via both 3D deconvolution of confocal image stacks and EM for *norpA, trp;trpl, hdc,* and *synaptotagmin* mutant eyes (see Supplemental Data). Again, we observed no morphological differences between the wild-type and any of the mutants (Figures 1D and 1E and Figure S2). For these analyses, we utilized

the crystalline array of photoreceptor terminals and cartridges to detect pattern alterations. However, it is conceivable that a mutant could harbor always six photoreceptors per cartridge, yet with incorrect subtype complements. To test this possibility, we utilized a marker for only one of the six subtypes, R4, during visual map formation [23]. We chose the *trp;trpl* double mutant for this analysis, because the *trp* and *trpl* channels are the final output components of the phototransduction cascade and are not only required for evoked activity [15] but also exhibit a lack of spontaneous activity in excised patch recordings from adult double mutant rhabdomere membranes [16]. As shown in Figure S3, the mutant exhibits a highly regular R4 projection pattern during visual map formation with a single, correctly positioned process per developing cartridge that is indistinguishable from wild-type. Finally, it is yet conceivable that every cartridge contains the correct complement of exactly one R1–R6 per cartridge, but that those are visuotopically incorrect. This would, for example, be the case if always precisely the R1–R6 from a single ommatidium were sorted into the same cartridge and thus were not sorted according to the principal of neural superposition. To test this possibility, we performed single-ommatidium DiI labelings [24]. We injected fluorescent dye into single ommatidia of wild-type and *trp;trpl* mutants and traced extending axons from the eye into the brain. In wild-type animals, R1–R6 axons from a single ommatidium extend into the brain in a single axon fascicle, and when they reach the developing

lamina, select targets arranged in an invariant relative pattern. This stereotyped pattern of innervation is preserved in axons from injected ommatidia in *trp;trpl* double mutant animals (Figures S3C and S3F; n = 8). Although we have not tested the possibility that *trp;trpl* mutant photoreceptors might choose wrong cartridges in competition with wild-type photoreceptors, we show that *trp;trpl*-dependent activity in R1–R6 is not required to form a morphologically normal visual map. For example, activity between photoreceptors during sorting may serve as a corrective mechanism of minor targeting errors and thereby increase the plasticity of the developing visual map. This possibility would be consistent with our finding that a complete lack of activity does not cause obvious defects. However, it would predict that in an experiment where certain aspects of neuronal activity were increased or decreased in individual photoreceptors, competition may lead to sorting defects. We do not think that this scenario is likely but want to stress that it is not formally tested in this study. In summary, we find no evidence for a requirement of evoked or spontaneous neuronal activity in axon targeting and terminal sorting according to the principal of neural superposition.

If neuronal activity were required to refine synapse numbers after axon targeting, we would expect quantitative and/or qualitative ultrastructural changes among the synapses. Each R1–R6 photoreceptor forms ∼50 evenly spaced synapses with postsynaptic lamina neurons [8, 10]. In the wild-type lamina of a newly emerged fly, we find on average ∼0.8 synaptic profiles per terminal in any given ultrathin section (Figure 1F). If synapse numbers were refined or "sculpted" in an activity-dependent fashion, we would expect some deviation from this number, or in the size of synaptic profiles, in the mutants. However, although we observed ultrastructural alterations in some mutants (e.g., the loss of synaptic vesicles in *synaptotagmin* and an increase in glial invaginations in *trp;trpl*), the number and composition of synaptic profiles proved to be highly constant (Figures 1F and 1G; Figure S4 and data not shown). Thus, in addition to axon targeting, terminal sorting, and filopodial fine structure, we find no evidence that photoreceptor terminals require evoked or spontaneous electrical activity or neurotransmitter release to form a precise number of morphologically normal synapses.

Cartridge Formation Is Sensitive to Mutational Perturbation and Predetermines Synaptic Partners

The activity-dependent sculpting of synapse numbers in the vertebrate visual system exemplifies how a neuronal circuit can be shaped *after* an initial phase of exuberant synaptogenesis. If such "postspecification" does not occur in *Drosophila* visual map formation, we have to postulate the existence of an intrinsic developmental program that ensures correct partner selection *prior* to (or *during*) synaptogenesis. The results of our activity disruption experiments are not consistent with activity-dependent postspecification, yet how can we provide positive evidence that synapses are prespecified in the fly's visual map? We know that each fly R1–R6 terminal forms a precisely regulated number of ∼50 synapses, or ∼300 per cartridge. However, it is not known whether this precise number is controlled cell autonomously by the photoreceptors themselves or in concert with the

postsynaptic cells in the cartridge. Activity-dependent regulation of synapse numbers in cartridges that faithfully represent neighboring points in visual space would require communication between pre- and postsynaptic cells. In contrast, the simplest activity-independent developmental program assuming correct partner selection prior to synaptogenesis would be the cell-autonomous determination of synapse numbers: the presorting of synaptic partners into cartridges could allow photoreceptors simply to form ∼50 synapses with any available postsynaptic partner in the cartridge. If this hypothesis is correct, any mutant causing R1–R6 to missort into cartridges, independent of the particular mutation or gene, should display an unaltered number of synapses per photoreceptor.

A precedent for counts of synapse numbers as a function of cartridge composition has been established for wild-type house flies [25]. To test the hypothesis of synapse constancy, we made use of a collection of mutants isolated in a large screen based on the *ey*FLP method [20, 26, 27] (Figure S5A). Among the mutants that affect cartridge composition isolated in this screen are the exocyst component *sec15* [20] as well as the receptor phosphatase *Dlar* [28, 29]. In addition to these two, we reasoned that if we can identify more mutants that cause R1–R6 to missort into cartridges, we can use these mutants to analyze synapse number as a function of cartridge composition independent of the genes affected by the mutations. In summary, we seek to uncover the developmental principles of how the visual map regulates synapse numbers by assessing how synapse formation depends on cartridge composition independent of the cause of cartridge missorting.

To understand the selection of mutants for this analysis, we first briefly provide relevant background information on their isolation. We first analyzed the 450 mutants of our collection with 3D confocal microscopy and subsequently carried out EM on 60 mutants. All mutants were selected based on a failure of photoreceptors to evoke a postsynaptic response [30], as monitored by electroretinograms (ERGs), without obviously affecting cell viability or phototransduction [20]. The failure to evoke a postsynaptic response could result from a defect either in neurotransmission, synapse formation, or synapse specification. Hence, the screen is designed to be sufficiently broad to target almost every aspect of synapse development. To analyze whether the mutants can indeed be utilized to identify critical developmental steps underlying visual map formation, we investigated the precise projection pattern of all mutants by 3D visualizations of photoreceptor-specific antibody labeling [31] (Figure S6). We first analyzed R1–R6 and R7/R8 targeting as well as R7 terminal pattern formation. In contrast to the neuronal activity mutants described above, approximately half of the mutants exhibited obvious patterning defects (Figure 2A). We defined three classes of morphological disruptions, in ascending order of their severity (Figure S6): class I mutants exhibit a disturbance of R7 terminals caused by filopodia overlapping between adjacent terminals, but no targeting defects with respect to neuropil layers; class II mutants are disrupted in R7/R8 target layer selection; and class III comprises mutants with pathfinding defects. Notably, our screen isolated mostly mutants with normal targeting but
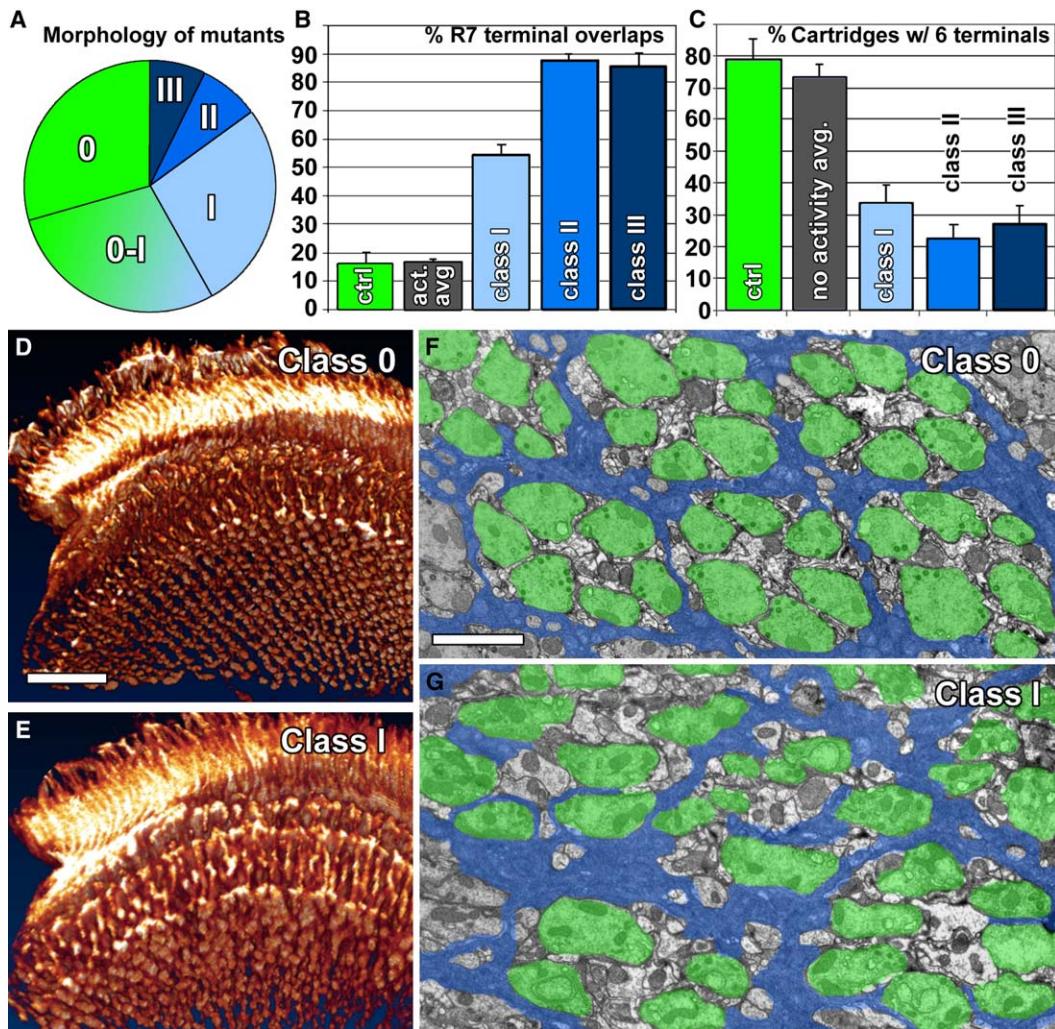
Figure 2. Forward Genetics: Novel Mutants Isolated in a Screen for Defects in Synapse Formation and Function Display Several Classes of Photoreceptor Projection Defects

(A) Distribution of mutants in different morphological classes as defined by 3D visualizations of photoreceptor projection patterns (cf. Figure S6). Class 0-I are mutants with possible subtle patterning defects that were not further analyzed.

(B) Quantification of R7 terminal fusions in 3D visualizations of the R7 terminal field reveal fusions between more than 50% of R7 terminals in class I mutants and more than 85% in class II and class III mutants. In contrast, the control as well as activity mutants display less than 20% R7 terminal fusions (cf. Figure 1C).
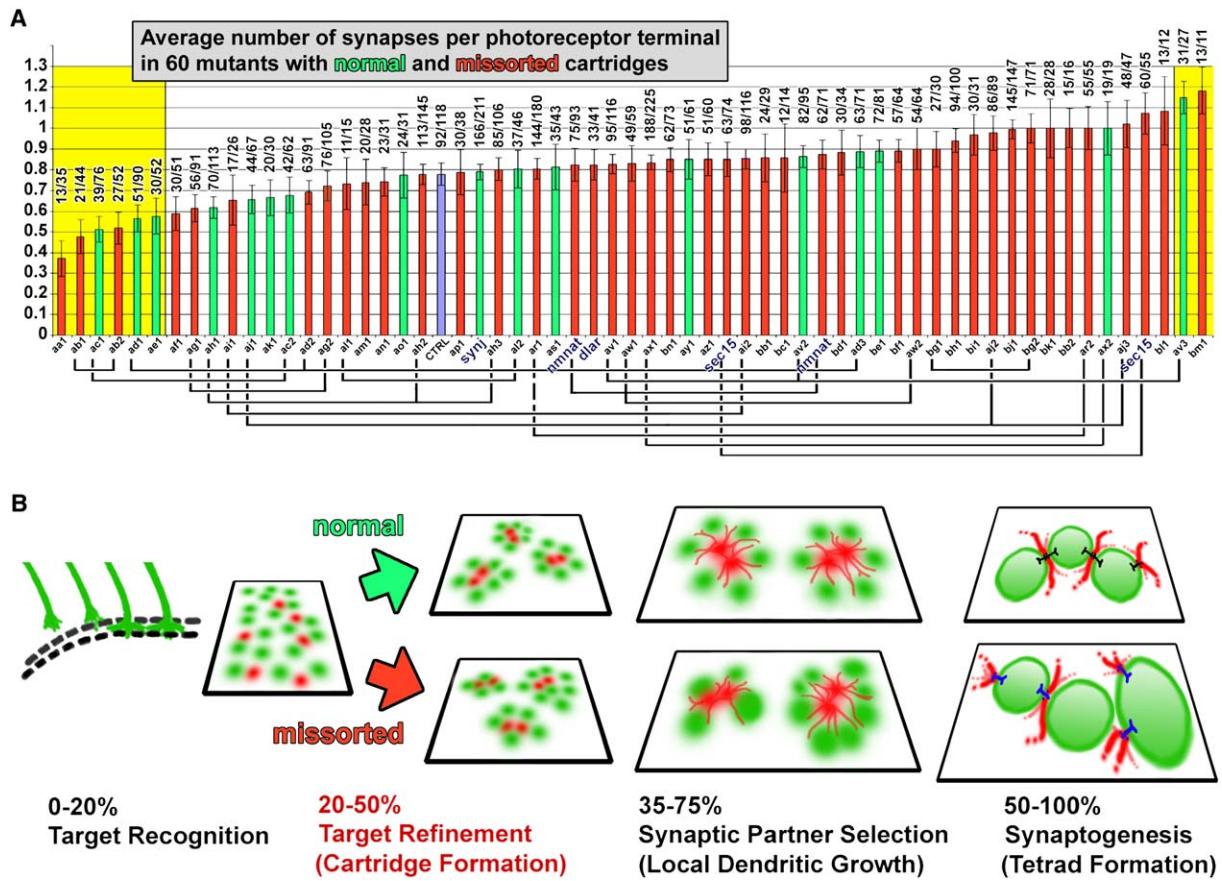
(C) In a functional visual map, six R terminals are clearly recognizable in 70%–80% of all cartridges. In contrast to control and activity mutants, class I–III mutants exhibit the correct number of R terminals per cartridge in less than 35% of all cartridges.

(D and E) Examples of class 0 and class I 3D visualization of photoreceptor projections and the R7 terminal field (cf. Figure 1B and Figure S6).

(F and G) Examples of electron micrographs of lamina cross-sections showing the normal organization of cartridges in a class 0 mutant (F) and cartridge missorting in a class I mutant (G). Photoreceptors are indicated in green, cartridge-insulating epithelial glia in blue. Error bars are SEM. Scale bars represent 20 μm in (D) for (D) and (E); 2 μm in (F) for (F) and (G).

obvious defects in terminal pattern formation (class I; Figures 2A, 2B, 2D, and 2E). The distribution of morphological classes is similar for all screened chromosome arms (Figure S5B), and the severity of morphological disruption correlates with the severity of the ERG phenotypes selected for in the screen (Figure S5C). Given the broad criterion of the primary screen, namely the failure to evoke a postsynaptic response, these data suggest that mutations in a surprisingly large number of genes specifically cause fine-structural disruptions, possibly at the level of synaptic partner selection or synapse formation, and that our screen strongly enriched for such mutants.

For an unbiased selection of mutants for our EM screen, we performed complementation analysis of all mutants and found a total of 64 complementation groups each with two or more alleles. We selected 60 mutants in 40 of these complementation groups that faithfully represent the distribution of morphological classes. Newly eclosed flies were fixed for EM to compare visual maps after development and before experience-dependent changes. Investigation of lamina cross-sections revealed that a surprising 75% (30 out of 40) of these complementation groups had defects in the sorting of R1–R6 terminals into cartridges, including *sec15* and *Dlar*, for which photoreceptor-targeting defects have been

Figure 3. Cartridge Sorting Is Highly Susceptible to Genetic Disruption, but Missorting Does Not Affect the Average Number of Synapses

(A) Quantitative ultratructural investigation of the average number of synapses per photoreceptor terminal in 60 mutants with normal (green) and missorted (red) cartridges. Control is shown in blue. Alleles of the same complementation groups are marked by connecting lines under the x axis. Mutants with synapse numbers that are significantly different from control are on yellow background (p < 0.01, two-tailed pairwise Student's t test of every mutant with control). Numbers above graphs show the exact number of synapses/terminals.

(B) Time series of developmental steps leading to the formation of visuotopically correct synapses. Neighboring cartridges are the synaptic units representing neighboring points in the visual world and form during the first half of brain development. The second half of brain development is characterized by synapse formation between synaptic partners that were prespecified during cartridge formation. A normal average number of synapses form in photoreceptor terminals independent of normal or missorted cartridge composition. Green, photoreceptor terminals; red, postsynaptic lamina monopolar cells.

Error bars represent SEM.

described previously [20, 28] (threshold criterion: <50% of cartridges contain six terminals; Figures 2C, 2F, and 2G; Figure S7). These findings indicate that the assembly of cartridges is highly susceptible to genetic disruption.

We next used the collection of 43 missorting mutants (corresponding to 30 complementation groups, including *Dlar* and *sec15*) to ask whether synapses form normally in such aberrant cartridges. In stark contrast to the large number of mutants with sorting defects, we found very few that affected either synapse number or composition, and none that lacked synapses (Figure 3A; Figure S7). As shown in Figure 3A, 52 out of 60 mutants, including 39 out of 43 missorting mutants, exhibit a normal average number of synapses per photoreceptor terminal (two-tailed pairwise Student's t tests of mutants with control). These findings are consistent with findings in mutants of the protocadherin *flamingo* [32], the exocyst component *sec15* [20], and manipulations that perturb cartridge sorting in house flies [33]. If the eight mutants with significantly more or fewer synapses than control (two-tailed pairwise Student's t test of every

mutant with control; yellow boxes in Figure 3A mark mutants with p < 0.01) were cases of reduced or increased synapse formation resulting from missorting, we should observe mostly mutants with missorting defects (red in Figure 3A) among them. We did not observe this. Importantly, our findings highlight the low variability of synapse numbers across the full range of mutants; however, this variability is likely to be even far lower because our analysis of only a single specimen per genotype in the EM screen should rather lead to an overestimation of the variability in synapse numbers. Additionally, for single specimens we make no claim about the statistical significance of synapse numbers in any particular mutant, but rather use the total distribution as an estimate of variation in synapse number in the presence of cartridge missorting. Finally, we checked synaptic sizes to ensure that these did not offset and thus hide possible changes in the numbers of synapses. Our measurement of synaptic profile size revealed significant differences only for mutants of two complementation groups (p < 0.01 in two-tailed pairwise Student's t test of every mutant
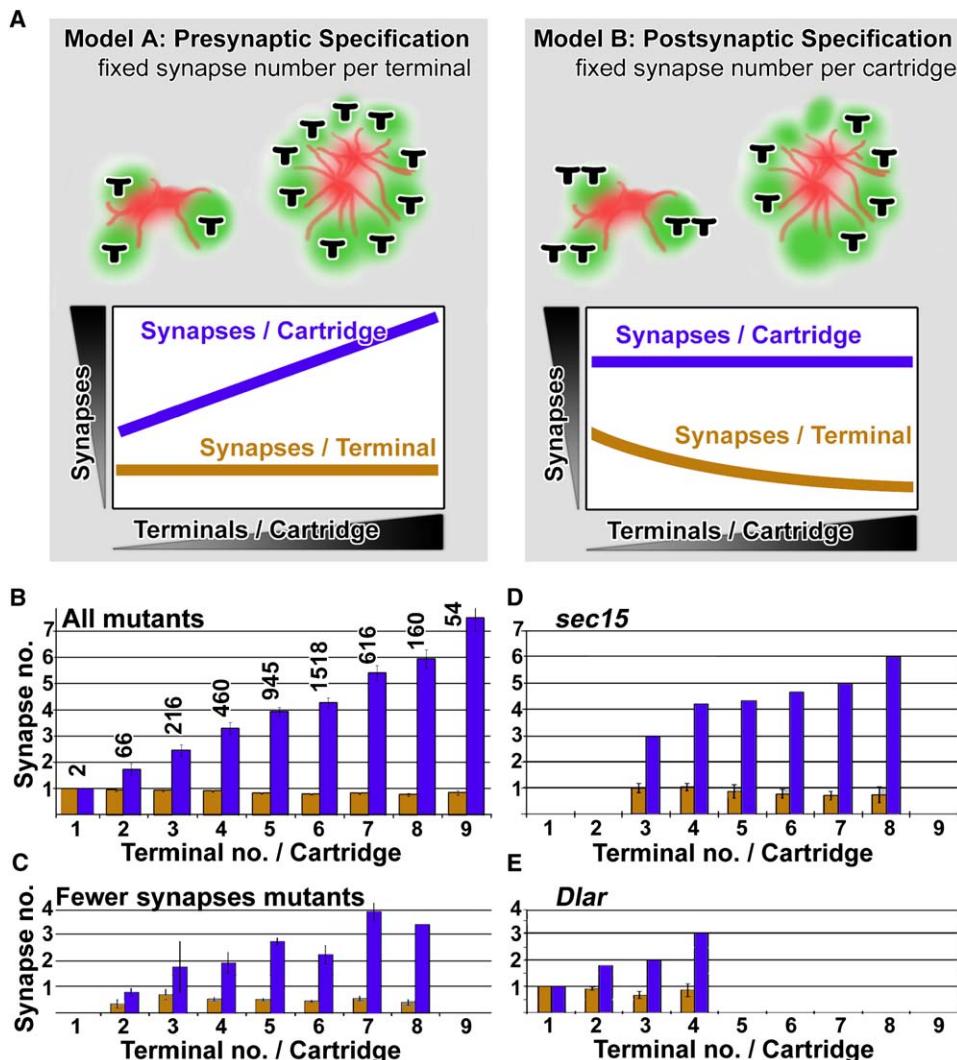
Figure 4. Synapse Constancy in Photoreceptors Suggests a Cell-Autonomous Intrinsic Developmental Program that Regulates Synapse Numbers

(A) Two models of synapse specification: in the case of presynaptic specification (model A), the number of synapses is constant per photoreceptor terminal, and therefore cartridges with more terminals contain more synapses; in the case of postsynaptic (or cartridge) specification (model B), the number of synapses per photoreceptor is variable and depends on the number of R terminals present in the cartridge.

(B) Synapse counts in a total of 4037 terminals in 783 cartridges with 1–9 terminals per cartridge reveals a fixed number of synapses per terminal independent of cartridge composition in agreement with model A. The number of synapses per terminal is shown in orange and is not significantly different for any cartridge composition (one-way ANOVA test; sample size is the number above each histogram bar [n = number of terminals]).

(C) The same plot as in (B) for mutants with significantly fewer synapses than control (cf. Figure 3A).

(D and E) Two mutants previously reported to display aberrant cartridge sorting and that we isolated in the screen: sec15 (D) and Dlar (E). Both are in agreement with model A, although in the case of Dlar the total number of terminals per cartridge is strongly reduced. For further plots of different electroretinogram mutant see Figure S9. Error bars are SEM.

with control), validating that our counts of synaptic profiles do indeed reflect numbers of actual synapses (Figure S8). These data therefore indicate that the formation of a correct average number of morphologically normal synapses in photoreceptors is independent of both correct cartridge composition and the specific mutations causing cartridge missorting (Figure 3B).

Precise Synapse Numbers Are Determined by Photoreceptors Independent of Cartridge Composition, Suggesting a Cell-Autonomous Developmental Program

Our analysis shows that a normal number of synapses can form between functionally inappropriate synaptic

partners (i.e., R1–R6 signaling divergent fields of view in missorted cartridges). However, we have not yet addressed which cells, pre- or postsynaptic, control the formation of such precise synapse numbers. Our collection of missorting mutants now allows us to test directly the hypothesis of synapse constancy. The observation of a normal average number of synapses per cartridge is compatible with both models (Figure 4A): either synapse numbers are controlled by the R1–R6 terminal independent of cartridge composition (model A, corresponding to the hypothesis of synapse constancy); or synapse numbers are controlled by the postsynaptic cells or the functional unit, the cartridge (model B, Figure 4A). Model A predicts the constancy of synapse

numbers per photoreceptor, resulting in varying numbers of synapses per cartridge in missorted cartridges; model B predicts the constancy of synapse numbers in cartridges, resulting in variable synapse numbers per photoreceptor terminal in missorted cartridges (Figure 4A). We tested these models by comparing numbers of synaptic profiles per R1–R6 terminal (n = 4038) and per cartridge (n = 783) in missorted cartridges. Hence, we counted the number of synapses as a function of cartridge composition in a total of 4038 terminals in 783 cartridges. Our counts for all 43 mutants with missorted cartridges reveal that the average number of synaptic profiles per cartridge positively correlates with the number of photoreceptor terminals in the cartridge (correlation coefficient = 0.995). Hence, in agreement with the hypothesis of synapse constancy (model A), the average number of synapses per R1–R6 is indeed constant, and missorting does not affect the regulation of synapse numbers in an individual photoreceptor terminal (Figure 4B). We further investigated whether this correlation fails when the mutants are compared in different subgroups: (1) mutants with reduced overall numbers of synapses (Figure 4C); (2) mutants affecting genes with known defects in cartridge formation: the receptor phosphatase *Dlar* [28, 29] (Figure 4E) and the exocyst component *sec15* [20] (Figure 4D); and finally (3) mutants that exhibit different classes of ERG defects (Figure S9). In all cases, the number of synaptic profiles per terminal is constant and independent of cartridge composition (all correlation coefficients > 0.99). We therefore conclude that each R1–R6 terminal forms synapses without regard to the number or identity of its neighboring terminals.

Our data show not only the normal numbers and structural composition of synapses between incorrect partners but further suggest that the precise number of synapses might be controlled by the photoreceptors and not by the postsynaptic neurons. To test this hypothesis unequivocally would require the identification of the precise complement of lamina cell types and numbers, as a function of photoreceptor terminal numbers in missorted cartridges. Such an analysis would require the analysis of serial EM reconstructions for a large number of missorted cartridges, a nearly impossible task. However, we identified two approaches to assess the lamina neuron complement in missorted cartridges based on our large mutant collection.

In the first approach we assumed that doubling the number of photoreceptor terminals or lamina neurons in a cartridge should on average result in a doubling of the corresponding areas in cartridge cross-sections. To quantify the pre- and postsynaptic areas in missorted cartridges, we first identified all mutants with identifiable cartridges, i.e., mutants where cartridge boundaries are not completely lost, and that revealed a pair of clearly discernible L1/L2 axon profiles in the center of the cartridge cross-section. These missorting mutants include photoreceptor terminal variability ranging from 2 to more than 8 terminals per cartridge and exhibit synapse constancy for photoreceptors just like all other missorting mutants. An example of such a missorting mutant is shown in Figure S10A. We then measured the complete areas of individual cartridges and subtracted from each one the area of all recognizable photoreceptor terminal profiles and obvious glial processes (black areas in

Figure S10B for the lamina region shown in Figure S10A). This analysis was performed for cartridges containing 2 to 8 terminals per cartridge. As shown in Figure S10C, while the total photoreceptor profile area per cartridge indeed doubles when the number of terminals doubles as predicted by our assumption (e.g., >5 μm^2 for cartridges with 2 terminals [2 T/C]; >10 μm^2 for 4 T/C; >20 μm^2 for 8 T/C [linear regression coefficient m = 3.17]), the nonphotoreceptor, nonglia profile area increases much less (e.g., 10 μm^2 for 2 T/C; 13 μm^2 for 4 T/C; 16 μm^2 for 8 T/C [linear regression coefficient m = 1.17]). This finding suggests that the number of postsynaptic lamina neurons does not change proportionally with the altered numbers of photoreceptor terminals in missorted cartridges. Instead, the much smaller increase in postsynaptic area in cartridges with more photoreceptor terminals likely results from the presence of a larger number of postsynaptic spines required to service the additional synaptic sites contributed by the increased number of presynaptic terminals. Indeed, the presence of split postsynaptic spine profiles was a criterion for our synapse counts.

To assess whether the postsynaptic area increase is indeed caused by spines, we demarcated only the clearly discernible central L1/L2 axons (depicted in red in Figure S10B). Indeed, these areas do not increase in size when the numbers of R1–R6 terminals per cartridge increase (Figure S10D; one-way ANOVA test). Postsynaptic profiles in control animals consistently occupy a smaller area than observed in missorting mutants. We speculate that in missorting mutants, more filopodial interactions are established or less are pruned after the complicated cartridge-sorting process. However, the comparisons of postsynaptic area profiles among missorting mutants with altered photoreceptor terminal complements are not affected by this observation. Our data suggest that photoreceptor terminal numbers can change in missorted cartridges independent of the main postsynaptic target cells. The observation that such photoreceptors still obey the rule of synapse constancy per photoreceptor terminal is most straightforwardly explained with a model in which synapse numbers are presynaptically specified. However, we have not ruled out that postsynaptic cells could still influence synapse numbers. A complementary experiment to the one presented here would be the assessment of synapse numbers in mutants with altered postsynaptic cell numbers but unaltered photoreceptor terminal numbers. However, in our collection of mutants, none recognizably exhibit such a phenotype. Hence, although the data provide support for our conclusion, we cannot fully rule out a role of the postsynaptic cells in influencing synapse numbers as long as the result of that influence is synapse constancy per photoreceptor.

Our proposed interpretation that the constancy of synapse numbers is controlled exclusively by the photoreceptor precludes the involvement of a postsynaptic feedback mechanism and the homeostatic regulation of synapse numbers. Homeostasis at the level of synaptic strength, i.e., a physiological compensation for the variability of synapse number per cartridge, is not excluded by our data. However, if such a mechanism exists, it could not compensate for the missorted input from different points in space and thus not correct the

visual map. Importantly, constancy of synapse numbers in spite of incorrect synaptic partner pairing is not consistent with either an activity-dependent or -independent refinement mechanism of synapse numbers and therefore corroborate our finding of normal synapse numbers in activity mutants. The model of synapse constancy provides positive evidence for the prespecification of synaptic partners in the fly's visual map.

Overall we interpret our results to indicate that synaptic specification is subdivided into three autonomous and genetically separable developmental steps. First, axonal pathfinding ends with the recognition of the correct neuropil layer. Second, sorting of R1–R6 between cartridges prespecifies synaptic partners. Third, after cartridge formation, each individual R1–R6 terminal forms a precise number of synapses within its cartridge independent of cartridge composition. Hence, the seemingly complex task of synapse specification in the *Drosophila* visual map is broken down into a series of simpler developmental steps. Our model thus reflects important differences from developmental events in forming vertebrate visual maps. First, axons from six photoreceptors that view a single point in visual space have to be sorted into a synaptic module in the fly lamina that represents that same point. In contrast, there is no corresponding prespecification step for the mapping of the much larger number of neighboring points in space by retinal ganglion cells in the vertebrate visual map; furthermore, the rough outline of that map is activity independent [1–3]. Hence, it is the fine-tuning or postspecification step that requires activity and distinguishes the tasks of forming vertebrate from fly visual maps. Second, the fly visual map must develop within a 4 day period of pupation, because the fly needs correct optomotor behavior almost immediately after eclosion. In contrast, activity-dependent fine-tuning typically extends postnatally in vertebrates. Furthermore, our model of a step-wise developmental program does not preclude posteclosion activity-dependent synaptic plasticity, which does not affect the wiring diagram of the visual map. Indeed, adult plasticity after the visual map is fixed has indeed been documented in the fly's visual system [34–36]. In contrast to the hard-wired visual map of the fly, activity-dependent refinement allows flexibility and plasticity of the visual map in vertebrates [2]. By contrast, to our knowledge, a role for neuronal activity in the formation of sensory maps or neural circuits has yet to be documented in the fly brain. In the olfactory system, Luo and colleagues have found prespecification of target neurons, leading them to conclude that the olfactory map is hard-wired [37]. Our data further support the notion that the *Drosophila* brain may to a large extent be hard-wired prior to eclosion. However, the extent to which precise synapse numbers are determined by activity-independent programs remains to be determined for other classes of synaptic contact, for other regions of the fly brain, and for more complex brains.

Experimental Procedures

Drosophila Strains, Mutagenesis, and Screen
Mutagenesis was performed as described [20, 27]. Of the 209,780 male flies screened for chromosome arm 2L, 2R, and 3R, 14,878 flies at least partly failed to phototax and were retained. In total, we established 457 stocks with an ERG defect; 374 are homozygous lethal. Complementation tests revealed 64 complementation groups with two or more alleles. Based on the consistency of phenotypes, 40 groups were selected for EM screen. For genotypes of activity mutants and experimental details on *para^{ts1}* heat shock and TTX injection experiments, see Supplemental Data.

Transmission Electron Microscopy and Quantification
EM was performed as described previously [27] on the laminas from *y w eyFLP;FRT40D mutation* (2L), *y w eyFLP;FRT42B mutation* (2R), or *y w eyFLP;FRT82B mutation* (3R). Flies carrying the unmutagenized isogenized chromosomes are used as control genotypes. For photoreceptor terminal and synapse quantification, photoreceptor terminals were identified by the presence of capitate projections, and synapses were identified by the presence of presynaptic dense bodies (T-bar ribbons) and a split postsynaptic side (at least two postsynaptic spine profiles) [9]. Standard errors for EM on single flies were calculated for n = the number of terminals counted for that genotype.

Immunocytochemistry, Image Acquisition, 3D Deconvolution, and Quantification
Adult brains were fixed in PBS with 3.5% formaldehyde for 15 min and washed in PBS with 0.4% Triton X-100. Antibody dilutions used [20]: anti-Chaoptin mAb24B10 1:50; anti-Sec6 1:2000; anti-Sec8 1:2000; anti-Ebony 1:200; secondary antibodies conjugated to Cy3, Cy5, or Alexa 488 (Jackson ImmunoResearch, West Grove, PA; Molecular Probes, Eugene, OR) were used at 1:250. All antibody incubations were performed at 4°C overnight in the presence of 5% normal goat serum. All fluorescent images were captured on a Zeiss LSM510 confocal microscope and processed with Amira 3.0 (TGS, Inc.) and Adobe Photoshop 7.0. 3D visualizations were generated with voltex visualization with Amira. Deconvolution was performed on 3D data sets with voxel sizes of 100 × 100 × 300 nm via a constrained blind deconvolution technique as described previously[38]. Only single confocal sections from 3D-deconvolved data sets are shown. R7 terminal overlaps were scored by quantifying the size of individual R7 terminals and the percentage of the overlapping area with neighboring terminals. Dye injections were performed as described previously [24].

Supplemental Data
Supplemental Data include ten figures and Supplemental Experimental Procedures and can be found with this article online at http://www.current-biology.com/cgi/content/full/16/18/1835/DC1/.

References

1. Shatz, C.J. (1996). Emergence of order in visual system development. Proc. Natl. Acad. Sci. USA *93*, 602–608.
2. Cline, H. (2003). Sperry and Hebb: oil and vinegar? Trends Neurosci. *26*, 655–661.

3. Chandrasekaran, A.R., Plas, D.T., Gonzalez, E., and Crair, M.C. (2005). Evidence for an instructive role of retinal activity in retinotopic map refinement in the superior colliculus of the mouse. J. Neurosci. *25*, 6929–6938.

4. Hua, J.Y., Smear, M.C., Baier, H., and Smith, S.J. (2005). Regulation of axon growth in vivo by activity-based competition. Nature *434*, 1022–1026.

5. Cang, J., Renteria, R.C., Kaneko, M., Liu, X., Copenhagen, D.R., and Stryker, M.P. (2005). Development of precise maps in visual cortex requires patterned spontaneous activity in the retina. Neuron *48*, 797–809.

6. Clandinin, T.R., and Zipursky, S.L. (2002). Making connections in the fly visual system. Neuron *35*, 827–841.

7. Kirschfeld, K. (1967). The projection of the optical environment on the screen of the rhabdomere in the compound eye of the *Musca*. Exp. Brain Res. *3*, 248–270.

8. Meinertzhagen, I.A., and Hu, X. (1996). Evidence for site selection during synaptogenesis: the surface distribution of synaptic sites in photoreceptor terminals of the flies *Musca* and *Drosophila*. Cell. Mol. Neurobiol. *16*, 677–698.

9. Meinertzhagen, I.A., and Hanson, T.E. (1993). The development of the optic lobe. In The Development of *Drosophila Melanogaster*, M. Bate and A. Martinez-Arias, eds. (Cold Spring Harbor, NY: Cold Spring Harbor Press), pp. 1363–1491.

10. Meinertzhagen, I.A., and Sorra, K.E. (2001). Synaptic organization in the fly's optic lamina: few cells, many synapses and divergent microcircuits. Prog. Brain Res. *131*, 53–69.

11. Lee, C.H., Herman, T., Clandinin, T.R., Lee, R., and Zipursky, S.L. (2001). N-cadherin regulates target specificity in the *Drosophila* visual system. Neuron *30*, 437–450.

12. Järvilehto, M., and Finell, N. (1983). Development of the function of visual receptor cells during the pupal life of the fly *Calliphora*. J. Comp. Physiol. [A] *150*, 529–536.

13. Hardie, R.C., Peretz, A., Pollock, J.A., and Minke, B. (1993). Ca2+ limits the development of the light response in *Drosophila* photoreceptors. Proc. Biol. Sci. *252*, 223–229.

14. Bloomquist, B.T., Shortridge, R.D., Schneuwly, S., Perdew, M., Montell, C., Steller, H., Rubin, G., and Pak, W.L. (1988). Isolation of a putative phospholipase C gene of *Drosophila*, *norpA*, and its role in phototransduction. Cell *54*, 723–733.

15. Niemeyer, B.A., Suzuki, E., Scott, K., Jalink, K., and Zuker, C.S. (1996). The *Drosophila* light-activated conductance is composed of the two channels TRP and TRPL. Cell *85*, 651–659.

16. Haab, J.E., Vergara, C., Bacigalupo, J., and O'Day, P.M. (2000). Coordinated gating of TRP-dependent channels in rhabdomeral membranes from *Drosophila* retinas. J. Neurosci. *20*, 7193–7198.

17. Hardie, R.C. (1987). Is histamine a neurotransmitter in insect photoreceptors? J. Comp. Physiol. [A] *161*, 201–213.

18. Burg, M.G., Sarthy, P.V., Koliantz, G., and Pak, W.L. (1993). Genetic and molecular identification of a *Drosophila* histidine decarboxylase gene required in photoreceptor transmitter synthesis. EMBO J. *12*, 911–919.

19. Koh, T.W., and Bellen, H.J. (2003). Synaptotagmin I, a Ca2+ sensor for neurotransmitter release. Trends Neurosci. *26*, 413–422.

20. Mehta, S.Q., Hiesinger, P.R., Beronja, S., Zhai, R.G., Schulze, K.L., Verstreken, P., Cao, Y., Zhou, Y., Tepass, U., Crair, M.C., et al. (2005). Mutations in *Drosophila sec15* reveal a function in neuronal targeting for a subset of exocyst components. Neuron *46*, 219–232.

21. Hiesinger, P.R., Reiter, C., Schau, H., and Fischbach, K.F. (1999). Neuropil pattern formation and regulation of cell adhesion molecules in *Drosophila* optic lobe development depend on synaptobrevin. J. Neurosci. *19*, 7548–7556.

22. Rister, J., and Heisenberg, M. (2006). Distinct functions of neuronal synaptobrevin in developing and mature fly photoreceptors. J. Neurobiol., in press.

23. Cooper, M.T., and Bray, S.J. (1999). Frizzled regulation of Notch signalling polarizes cell fate in the *Drosophila* eye. Nature *397*, 526–530.

24. Clandinin, T.R., and Zipursky, S.L. (2000). Afferent growth cone interactions control synaptic specificity in the *Drosophila* visual system. Neuron *28*, 427–436.

25. Frohlich, A., and Meinertzhagen, I.A. (1987). Regulation of synaptic frequency: comparison of the effects of hypoinnervation with those of hyperinnervation in the fly's compound eye. J. Neurobiol. *18*, 343–357.

26. Newsome, T.P., Asling, B., and Dickson, B.J. (2000). Analysis of *Drosophila* photoreceptor axon guidance in eye-specific mosaics. Development *127*, 851–860.

27. Verstreken, P., Koh, T.W., Schulze, K.L., Zhai, R.G., Hiesinger, P.R., Zhou, Y., Mehta, S.Q., Cao, Y., Roos, J., and Bellen, H.J. (2003). Synaptojanin is recruited by endophilin to promote synaptic vesicle uncoating. Neuron *40*, 733–748.

28. Clandinin, T.R., Lee, C.H., Herman, T., Lee, R.C., Yang, A.Y., Ovasapyan, S., and Zipursky, S.L. (2001). *Drosophila* LAR regulates R1-R6 and R7 target specificity in the visual system. Neuron *32*, 237–248.

29. Maurel-Zaffran, C., Suzuki, T., Gahmon, G., Treisman, J.E., and Dickson, B.J. (2001). Cell-autonomous and -nonautonomous functions of LAR in R7 photoreceptor axon targeting. Neuron *32*, 225–235.

30. Coombe, P.E. (1986). The large monopolar cells L1 and L2 are responsible for ERG transients in *Drosophila*. J. Comp. Physiol. [A] *159*, 655–665.

31. Fujita, S., Zipursky, S., Benzer, S., Ferrus, A., and Shotwell, S. (1982). Monoclonal antibodies against the *Drosophila* nervous system. Proc. Natl. Acad. Sci. USA *79*, 7929–7933.

32. Lee, R.C., Clandinin, T.R., Lee, C.H., Chen, P.L., Meinertzhagen, I.A., and Zipursky, S.L. (2003). The protocadherin Flamingo is required for axon target selection in the *Drosophila* visual system. Nat. Neurosci. *6*, 557–563.

33. Frohlich, A., and Meinertzhagen, I.A. (1993). Cell recognition during synaptogenesis is revealed after temperature-shock-induced perturbations in the developing fly's optic lamina. J. Neurobiol. *24*, 1642–1654.

34. Barth, M., Hirsch, H.V., Meinertzhagen, I.A., and Heisenberg, M. (1997). Experience-dependent developmental plasticity in the optic lobe of *Drosophila melanogaster*. J. Neurosci. *17*, 1493–1504.

35. Rybak, J., and Meinertzhagen, I.A. (1997). The effects of light reversals on photoreceptor synaptogenesis in the fly *Musca domestica*. Eur. J. Neurosci. *9*, 319–333.

36. Kral, K., and Meinertzhagen, I.A. (1989). Anatomical plasticity of synapses in the lamina of the optic lobe of the fly. Philos. Trans. R. Soc. Lond. B Biol. Sci. *323*, 155–183.

37. Jefferis, G.S., Marin, E.C., Stocker, R.F., and Luo, L. (2001). Target neuron prespecification in the olfactory map of *Drosophila*. Nature *414*, 204–208.

38. Hiesinger, P.R., Scholz, M., Meinertzhagen, I.A., Fischbach, K.F., and Obermayer, K. (2001). Visualization of synaptic markers in the optic neuropils of *Drosophila* using a new constrained deconvolution method. J. Comp. Neurol. *429*, 277–288.